New Resilience Index for Urban Water Distribution Networks

A NEW RESILIENCE INDEX FOR URBAN WATER DISTRIBUTION NETWORKS

G.P. Cimellaro[1], A.Tinebra[2], C.Renschler[3], M.Fragiadakis[4]

ABSTRACT

The increased frequency of natural disasters and man-made catastrophes has caused major disruptions to critical infrastructures (CI) such as Water Distribution Networks (WDNs). Therefore, reducing the vulnerability of the systems through physical and organizational restoration plans are the main concern for system engineers and utility managers that are responsible for the design, operation, and protection of WDNs. In this paper, a Resilience Index (R) of a WDN has been proposed which is the product of three indices: (i) the number of users temporary without water, (ii) the water level in the tank, and (iii) the water quality. The Resilience Index is expected to help planners and engineers to evaluate the functionality of a WDN which includes: (1) delivering a certain demand of water with an acceptable level of pressure and quality; (2) the restoration process following an extreme event. A small town in the South of Italy has been selected as a case study to show the applicability of this index using different disruptive scenarios and restoration plans. The numerical results show the importance of the partition of the network in districts to reduce the extension of disservices. It is also shown the necessity to consider the indices separately to find trends that cannot be captured by the global index. Advantages and disadvantages of the different restoration plans are discussed. The proposed indices can be implemented in a decision support tool used by governmental agencies which want to include the restoration process, the environmental and social aspects in their design procedure.

KEYWORDS**:** Water Distribution Network, Disaster Resilience, Recovery, Resilience, Restoration, Seismic Risk, Resilience index, Vulnerability, Infrastructure, Restoration Strategies

INTRODUCTION

[1] Visiting Professor, Department of Civil and Environmental Engineering, University of California Berkeley, Davis Hall, Berkeley, CA 94720-1710, USA (gianpaolo.cimellaro@polito.it)
[2] Graduate Research Assistant, Department of Structural and Geotechnical Engineering (DISEG), Politecnico di Torino, 10129 Turin, Italy (gianpaolo.cimellaro@polito.it)
[3] Associate Professor, Department of Geography, University at Buffalo (SUNY), 116 Wilkeson Quad, Buffalo, NY 14261, U.S.A. email: rensch@buffalo.edu
[4] Lecturer, School of Civil Engineering, National Technical University of Athens, email: mfrag@mail.ntua.gr

The water distribution networks and the Critical Infrastructures (CI) in general provide services by allowing flows of fuels, materials, information, electric power etc.. The *disruptions* change the operability state of parts of the network (e.g. nodes and/or links), and then the *recovery actions* restore the functionality of the damaged parts of the network, allowing the performance of the system to return to the nominal levels as fast as possible. In the past, emphasis was given to the physical protection of water distribution networks, but now attention is shifting toward the infrastructure resilience, defined as the ability of infrastructure systems to withstand, adapt to, and rapidly recover from the effects of a disruptive event. This concept is becoming increasingly important in the context of CIs and defining infrastructure functionality is essential for evaluating its resilience (Cimellaro et al., 2014a). Although several authors (Holling, 1973; Mileti, 1999; Fiksel, 2003) have worked in the field of Disaster Resilience, Bruneau et al. (2003) offered the first broad definition of this quantity including the effects of losses, mitigation and rapid recovery. In their study, they identify four dimensions of community resilience, namely: i) *technical*, ii) *organizational*, iii) *social*, and iv) *economic*. However, in their work they did not provide a detailed quantification of it, but rather a collection of quantitative performance criteria for each property. After the general framework provided by Bruneau et al., various studies have been carried out, with the goal of evaluating resilience and identifying its main units of measurement. For example, Cimellaro et al. (2005, 2010a), formulated the first framework to quantify resilience, where uncertainties in the intensity measures were considered. Chang and Shinozuka (2004) refined the method proposed by Bruneau (2003), by proposing a metric of system performance *Q*, which is evaluated comparing the extreme events scenario with the normal operating conditions and they applied the method to the case study of the Memphis water system. Miles and Chang (2006) presented a comprehensive conceptual model of recovery, which establishes the relationships between a community's household business, lifeline networks and neighborhoods. Even if a measure of resilience

47 is not provided in their work, the paper points out the necessity to correlate the concept of recovery to
48 real factors, such as household income, the year the structure was built, etc.. The same year Cagnan et
49 al. (2006) has developed a model of post-earthquake restoration processes for an electric power system.
50 A discrete event simulation model based on available data has been built, with the goal of improving the
51 restoration processes in future earthquakes.
52 Several authors have used the resiliency concept as input in *decision support methodologies* that assist
53 authorities in prioritizing infrastructure investments for disaster mitigation, emergency response and
54 recovery activities. In particular, it has been applied to *hospitals* (Cimellaro et al., 2010b; Cimellaro and
55 Pique`, 2014a), *lifeline structures* (Ouyang and Duenas-Osorio, 2011, Cimellaro et al., 2014b; Ouyang,
56 2014) and *cities* (Chang et al, 2014) using different optimization methods based on *economic* (Chang
57 and Shinozuka, 2004), *downtime* (Cagnan et al., 2006) or *multi-criteria analysis* (Javanbarg et al., 2008).
58 Recently Cimellaro et al. (2014c) have developed a new methodology to evaluate resilience on physical
59 infrastructures including their interdependencies using time series analysis and applying it to the 2011
60 Tohoku earthquake in Japan.
61 According to the literature, several methods are available for quantifying resilience of infrastructure
62 systems which can be grouped in *probabilistic methods* (Miller-Hooks et al, 2012, Queiroz et al., 2013),
63 *graph theory methods* (Berche et al, 2009; Leu et al., 2010, Dorbritz, 2011), *fuzzy methods* (Heaslip et
64 al., 2010) and *analytical methods* (Cimellaro et al., 2010; Tamvakis and Xenidis, 2013).
65 Miller-Hooks et al. (2012) proposed a non-linear, stochastic program addressing an integer L-shaped
66 method associated with Monte Carlo simulations to quantify resilience. However, the method is
67 computationally unaffordable for real systems which include a large number of interdependent nodes.
68 Dorbritz (2011) combined the approach of Bruneau et al. (2003), with network analysis and proposed a
69 resilience quantification method that tries to introduce, also, the complex network concepts introduced

by Berche et al. (2009) for the public transportation network. Heaslip et al. (2010) developed a method to assess and quantify resilience using Fuzzy Inference Systems (FIS). In particular, they developed a hierarchically structured dependency diagram of variables that can represent the performance hierarchy levels. However, the use of more intuitive values for variables that quantify resilience may have an effect on the accuracy of assessments and may complicate the decision making process. Furthermore, a complete FIS should include a large number of variables and rules which might make the method computationally unaffordable. Recently, Tamvakis and Xenidis (2013) proposed a framework based on entropy theory concepts. Entropy describes the system's disorder at a given point in time and it is measurable in a single metric analogously to resilience which describes the system's potential to recover to a desired system's condition. Although the idea seems promising, they fail to provide details about the method and applications which show the feasibility of the methodology.

When considering the *reliability of infrastructures*, the different methodologies available in literature can be grouped in two main categories: (i) *simulation-based models* and (ii) *analytical methods* (Kim et al., 2010). (i) Simulation-based models involve the use of random sampling techniques and Monte Carlo simulation to approximate system functionality. For example, Wang and O-Rourke (2008) characterized the performance of a large water supply system in term of system reliability and serviceability. They use probabilistic seismic hazard analysis, theoretical and empirical relations to estimate pipeline response. (ii) Analytical methods do not require repeated sampling and therefore they allow more rapid computations, but they are based on assumptions that sometimes might not fit to the problem at hand (Francis and Bekera, 2014; Davis, 2014).

In the last decade, several metrics have been proposed in literature to measure the performance of WDNs. A good state of the art is available in Jalal (2008). For example, Todini (2000) proposed an index which is a measure of the capability of the network to cope with failures and it is related indirectly

93 to system reliability. Other authors have also extended this resilience index to overcome certain
94 drawbacks (Prasad and Park, 2004; Jayaram and Srinivasan, 2008), such as the inapplicability of the
95 index in networks with multiple sources. They have listed the theoretical advantages of their
96 approaches, but none of them has compared the performance of these resilience indices. Recently,
97 Davis (2014) in his work has defined 5 categories of water services. He has compared pre and post-
98 disaster services and has distinguished between operability and functionality. Of course, the literature
99 review presented above cannot be comprehensive, but many of the works cited are based on the review
100 of previous works to quantify resilience, therefore it is still adequate to identify the different trends to
101 quantify resilience of infrastructures.

102 In this study, a Resilience Index (R) for a water distribution system has been proposed to measure
103 its performance. The proposed index R is defined as the product of three indices: one describes the
104 demand and is based on the number of users temporary without water (R_1); the second describes the
105 capacity and is based on the tank water height (R_2); the third (R_3) is based on the water quality. These
106 indices will help planners and engineers to evaluate the functionality of a water distribution system
107 which consists in delivering a certain demand of water with an acceptable level of pressure and quality.
108 A small town located in a seismic region in Italy, has been used as a case study. The WDN has been
109 analyzed using the software EPANET 2.0 (Rossman, 2000) and different restoration plans have been
110 compared using the proposed resilience indices.

111 **RESILIENCE OF WATER DISTRIBUTION NETWORK**

112 The definition that has been used in this paper to quantify resilience of the WDN is the one provided in
113 the work of Bruneau et al. (2003) where resilience is defined as the *ability of a system to reduce the*
114 *chances of shock, to absorb such a shock if it occurs and to recovery quickly after a shock*. Later the
115 same definition has been quantified and extended by Cimellaro et al. (2010a, b), where the resilience

index (R) has been defined as *a function indicating the capability to sustain a level of functionality for a given building, bridge, lifeline networks, or community, over a period defined as the Control Time (T_{LC}) that is usually decided by owners, or society (e.g. life cycle of the system, etc.)*. An essential parameter for the definition of Resilience of the WDN is the definition of functionality/performance index which is provided in the next paragraph.

Definition of a new performance index for Water Distribution Networks

Earthquake effects on water supply systems have been investigated extensively in literature and different methodologies for estimating the reliability and serviceability of water supply systems heavily damaged by earthquake are available in literature (Ballantyne et al., 1990; Taylor, 1991; Shinozuka et al., 1992; Markov et al., 1994; and Hwang et al., 1998). The proposed index is composed of three parts which depend on the number of households that would suffer water outage, the tank water level and the water quality. The first part of the index is proportional to the system serviceability index (SSI) proposed by Todini (2000), which is defined as the ratio of the sum of satisfied water demands after an earthquake to that before an earthquake. In detail, three performance functions $F_1(t)$, $F_2(t)$ and $F_3(t)$ have been presented. $F_1(t)$ relates to the number of households without water, therefore it is related to the *social dimension* of the resilience problem. Analytically it is defined as

$$F_1(t) = 1 - \frac{\sum_i n_{p,e}{}^i}{n_{Tot}} \quad \text{for } i = 1 \ldots n \tag{1}$$

where $n_{p,e}{}^i$ are the equivalent number of users for each node that suffer insufficient pressure, n_{Tot} are the total number of users within the distribution system, n is the total number of nodes that suffer water outage. The Loss Function $L_1(I,T_R)$ is defined as

$$L_1(I,T_R) = \frac{\sum_i n_{d,e}{}^i (I,T_R)}{n_{Tot}} \quad \text{for } i = 1 \ldots n \tag{2}$$

where $n_{d,e}^{i}$ are the number of *Demand Nodes* which are assumed directly proportional to the water volume lost W_{Lost} during the extreme event and the repair operations; I is an intensity parameter; T_R is the recovery period which is defined as the period necessary to restore the functionality of a system to a desired level that can operate or function the same, close to, or better than the original one (Cimellaro et al, 2010). In detail, $n_{d,e}^{i}$ is given by the following equation

$$n_{d,e}^{\ i} = n_i \cdot \frac{W_{Lost}^{\ i}}{W_i} \tag{3}$$

where i indicates the general node in which the pressure is insufficient to ensure the demand water flow; n_i is the total number of entities connected to node i; W_{Lost}^{i} is the water volume lost and W_i is the water volume that the entities would consume in normal operating conditions. To evaluate the volume of water lost and the volume of water in normal operating conditions, the following equations have been used

$$W_i = \int_{t_j}^{t_{j+1}} Q_{Demand}(t)dt \tag{4}$$

$$W_{Lost}^{\ i} = \int_{t_j}^{t_{j+1}} [Q_{Demand}(t) - Q_i(t)]dt \tag{5}$$

where t_j and t_{j+1} are generic instants after the extreme event ($t > t_1$); Q_{Demand} is the water demand flow at the instant t and Q_i is the real water flow at the time t afterwards the damage of the pipe. For a given extreme event, the general form of $F_1(t)$ is shown in Figure 1a. The control time T_{LC} has been divided in four different period ranges. $T_{NF\text{-}I}$ is the normal operating functionality period before the earthquake; T_M is the operating period range immediately after the earthquake and before the first emergency operations; T_E is the transition period when the water system is partially in service; $T_{NF\text{-}II}$ is the normal operating functionality after the repair operations. Moreover, t_1 is the time instant when the extreme event occurs, t_2 is the time instant when the damaged pipe is isolated, t_3 is the time instant when the repair operations are finished and t_4 is a generic instant when the system works in normal operating

158 conditions. The difference between t_3 and t_1 corresponds to the Recovery Time T_R. Then the restoration
159 process has been divided in two phases: *Phase I* is the time interval necessary for the first emergency
160 operations and the isolation of the area where the damage happens, while *Phase II* is the time interval
161 necessary for the repair operations. During *Phase II*, the users are temporary without water, so, in this
162 case, the water flow is equal to zero, while the ratio $W_{Lost}{}^{i}/W_i$ is equal to 1, since $n_e{}^{i} = n_i$. Therefore,
163 after the definition of the performance index $F_1(t)$ given in Equation (1) the corresponding resilience
164 index is defined as

165 $$R_1 = \int_0^{T_{LC}} \frac{F_1(t)}{T_{LC}} dt \qquad (6)$$

166 where $F_1(t)$ is the performance function proportional to the number of equivalent households n_e w/o
167 service; T_{LC} is the control time.
168 The second performance function $F_2(t)$ relates to the tank water level, which is directly related to the
169 reserve capacity of the tank and therefore to the *technical dimension* of the resilience problem. The
170 analytical expression is defined as

171 $$F_2(t) = \begin{cases} \dfrac{h(t)}{h_{\mathrm{Re}serve}} & h \le h_{\mathrm{Re}serve} \\ 1 & h > h_{\mathrm{Re}serve} \end{cases} \qquad (7)$$

172 where $h(t)$ is the water level in the tank at a given instant of time, while $h_{Reserve}$ corresponds to the
173 reserve capacity in the tank. In detail, if the water level is above the height corresponding to the reserve
174 capacity $h_{Reserve}$, $F_2(t)$ is equal to 1, but if the level decreases below $h_{Reserve}$, $F_2(t)$ has a value less than 1.
175 In this case, the Loss Function $L_2(I, T_R)$ is given by

176 $$L_2(I, T_R) = 1 - \frac{h(t, I, T_R)}{h_{\mathrm{Re}serve}} \qquad (8)$$

177 The loss function given in Equation (8) provides information about how much water has been lost
178 during the earthquake and allows establishing what is the optimal strategy to recover the Reserve
179 Capacity.
180 The definition of performance function in equation (7) can be generalized and extended not only to
181 tanks, but also to pumps, by using the "Hydraulic head" or "Piezometric head" which is a specific
182 measure of liquid pressure that can also be used for pumps.
183 With respect to Equation (2), for Equation (8) is not possible to define a fixed recovery time before the
184 numerical simulations, because in this case T_R is directly related to the type of restoration plan adopted.
185 In Figure 1b is shown a sketch of how $F_2(t)$ looks like. The figure shows how $F_2(t)$ doesn't return to 1 at
186 the end of T_{LC} , but it can assume lower values, if a proper restoration strategy is not adopted. In this
187 case, the Resilience Index is given by

188 $$R_2 = \int_0^{T_{LC}} \frac{F_2(t)}{T_{LC}} dt \qquad (9)$$

189 where $F_2(t)$ is the water level in the tank; T_{LC} is the control time. Special attention requires the
190 definition of R_2 when multiple tanks are in the network. In this case, the index is given by

191 $$R_2 = \frac{\sum_i w_i R_2^{\,i}}{\sum_i w_i}; \quad i = 1,2 \qquad (10)$$

192 where w_i are the weight coefficients of the n tanks in the network. These coefficients can be evaluated
193 using two approaches. Assuming two tanks, in the first case, the weights w_1 and w_2 are proportional to
194 the average flow loss on the two pipes in which the connecting pipe is divided after the earthquake. In
195 the second case, the weights w_1 and w_2 are proportional to the reserve capacity.
196 Since WDNs have strict requirements of ensuring water quality, the global resilience index should also
197 include a water quality index which is related to the *environmental dimension* of the resilience problem.

198 Currently there is no globally accepted composite index of water quality. Most water quality indices rely
199 on normalizing, or standardizing data according to expected concentrations and some interpretation of
200 'good' versus 'bad' concentrations. Parameters are often then weighted according to their perceived
201 importance to overall water quality and the index is calculated as the weighted average of all the
202 observations of interest. The authors do not want to enter in the discussion of which index is better to
203 adopt, however once an index of water quality check Q is selected, it can be compared with its value
204 before the earthquake event defining the following performance function

205 $$F_3(t) = \frac{Q(t)}{Q^*} \tag{11}$$

206 where Q^* and $Q(t)$ are the water quality indices before and after the seismic event respectively. The
207 final resilience index for water quality is defined as

208 $$R_3 = \int_0^{T_{LC}} \frac{F_3(t)}{T_{LC}} dt \tag{12}$$

209 Then the three indices are combined together to have a comprehensive evaluation of the WDN, so the
210 Global Resilience Index is defined as

211 $$R = R_1 \bullet R_2 \bullet R_3 \tag{13}$$

212 The R index summarizes the performance of the WDN considering the demand R_1 (users), the capacity
213 R_2 (water level in the tank) and the water quality R_3.
214 The metrics has been multiplied, because the global index R in equation (13) is more sensitive to the
215 different scenario events when the three indices are multiplied. In fact some scenarios in the case study
216 below generate high values of R_1, so it seems that damage did not cause any effect, but in reality the
217 quantity of water loss has been relevant and this cause a reduction of the water reserve capacity in the
218 tank and consequently of R_2.

CASE STUDY

The methodology described above has been applied to the WDN of Calascibetta, an italian town supplying 4600 inhabitants in the Enna Province, located on Erei Mountains (Figure 2) in Sicily.

Seismic hazard in the region

The town did not suffer high intensity earthquakes except the '*Noto valley earthquake'* which occurred in 1693 and produced severe damages in the entire eastern side of the island. Its intensity was about *XI° of Mercalli–Cancani–Sieberg (MCS)* scale, but in Calascibetta the intensity felt was about *VII°*. Using the Neo-deterministic seismic hazard scenario proposed by Panza et al. (2012), the value of the peak ground velocity in the town of Calascibetta (14.4000 N 37.4000 E) is in the range between 15 and 30 cm/sec (Panza et al., 2014a). The Neo-determinist approach has been preferred with respect to the Probabilistic Seismic Hazard analysis (Cimellaro et al., 2011), because the former provides non conservative results (Panza et al., 2014b) at the specific site. The PGV used in the analysis is the average value of 22.5 *cm/s*, which can be assumed constant over the entire WDN, because of the limited extension of the network.

Characteristics of the water distribution network

The WDN consists of two tanks:

1. the *roof tank* (Capacity = 50 m^3) located in the highest part of the town;
2. *St. Peter's tank* (Capacity = 500 m^3), which is supplied by the pipes coming from the roof tank.

The water source capacity of the two tanks is the reservoir located at Ancipa Dam. The water is pumped at the roof tank from a station located at the bottom of the hill and from there, the water is distributed to district 1 and to St. Peter tank which supplies the entire city. The paper deals only with the distribution network, while the adduction network in not considered in the analysis. The entire network is made by

243 polyethylene pipes which are characterized by an easy process of installation, high elasticity that allows
244 it to absorb modest land subsidence without damage on the structure, chemical inertness against the
245 aggressiveness of land or percolated water or liquids conveyed. In
246 Figure **3** is shown the plan view of the WDN of Calascibetta which is divided in eight districts. All
247 districts are connected through pipes which are normally closed in normal operating conditions, but they
248 can be open in case of an emergency. Three diameters of respectively 63, 110, 160 *mm* are installed in
249 the network, while 32 *mm* diameter pipes have been used to connect the different services within the
250 building.
251 The length of the 32, 63, 110 and 160 mm diameter pipes are respectively 3728.83m, 8719.35m,
252 4427.65 and 1115.35m. Pressure reducing valves (*PRV*) have been installed in the network to maintain
253 the pressure within certain limits which are given in Table 1, while shut-off valves have been installed to
254 close the pipes in case of an emergency (
255 Figure **3**).
256
257 **Model description, assumptions and calibration**
258 The WDN of Calascibetta has been modeled using EPANET 2.0 (Rossman, 2000). The standard
259 procedure used in the software to evaluate the nodes' pressure and the flow in each pipe is the Demand
260 Driven Analysis (*DDA)*. However, the limitation of this method is that the demand flow is fixed a priori
261 in each node, so the DDA provides the same value of demand flow even if the pressure is below the
262 threshold necessary to satisfy the demand in the WDN. For these reasons, the DDA works well in
263 normal operating conditions when there are no failures in the pipes, but if one pipe fails, the pressure in
264 some nodes could be below the threshold value necessary to satisfy the demand. In this case, the
265 Pressure Driven Analysis (PDA) has been used. So all the simulations with pipe failures start with a

DDA analysis and when the pressure in one node goes below the threshold necessary to satisfy the demand flow, it is transformed in a *Emitter* node (Rossman, 2000). The PDA analysis in presence of Emitters is characterized by less flow circulating in the network and consequently by reduced hydraulic head losses when compared with the first analysis (DDA). In the analysis, the pressure necessary to satisfy the demand flow at each node is set to 20 *m* of water column (2 *bar),*so that at least 5 *m* of water column are above the tallest house in Calascibetta which has an height of about 13 m. The *Darcy-Weisbach* formula has been used to evaluate the head losses which are given by

$$h = \lambda(\varepsilon, d, q)\frac{L \cdot v^2}{d \cdot 2g} \qquad (14)$$

where λ is the friction factor (depending on the roughness ε, the diameter d and the flow rate q), L is the pipe length, v is the flow velocity, g is the acceleration of gravity. The friction factor λ is estimated with the use of different equations as a function of the *Reynolds Number* (*RE*). The roughness ε for the polyethylene pipes has been assumed constant and equal to 0.005 *mm*, because the pipes have been recently installed and in general, the polyethylene material maintains its hydraulics characteristics. The concentrated losses have been neglected. Pipes with the same features (e.g. diameter, roughness) have been combined into a single pipe with length equal to the sum of the lengths of each pipe. The pipes with diameter of 32 *mm* connecting to the services have been neglected. The roof tank has a cylindrical shape with a diameter of 3 m, while St.Peter tank is composed by two tanks of rectangular shape that cover an area of 66 m^2 each. To simplify the modeling in EPANET the rectangular tank has been replaced with an equivalent tank with a diameter of 12.95m that have a cylindrical shape of the same volume ($D = \sqrt{4A/\pi} = \sqrt{4 \cdot 132/\pi} \cong 12.95m$). The variation of water flow demand over the 24 hours has been determined using the data provided from the operator from *July 2011* to *June 2012*. In particular, the water flow demand is obtained as average of a monthly time pattern for each district. For example, Figure 4 shows the water flow demand related to District 1. Pipe breaks and leaks have been modeled

289 in EPANET using the scheme shown in Figure 5, however simulations have been focusing only on pipes
290 breaks which are assumed to happen in the middle point of the pipe. Then at the end-parts of the
291 divided pipe, two reservoirs are added to simulate the water flow through the crack. The tanks have a
292 hydraulic head equal to the elevation of the break point which is evaluated with a linear interpolation
293 between the two nodes of the original pipe. Finally, a valve is inserted on each new pipe so that the
294 water can only flow from the broken pipe to the tanks and not vice versa.
295
296 **Seismic Damage Model for water pipes**
297 Pipeline damage models for the seismic vulnerability assessment are usually formulated as the repair
298 rate for unit length of pipes. These models can be derived from the data collected during previous
299 seismic events or any other hazard which produced breakages in the pipes. In this research, the well
300 known model in the American Lifeline Alliance (ALA, 2001) has been used. In particular, the repair rate
301 is defined as
302 $$RR = K(0.00187)PGV \quad (15)$$
303 where *RR* is the Repair Rate which is the number of pipe breaks per 1000 *ft* (305 m) of pipe, *K* is a
304 coefficient determined by the pipe material, pipe joint type, pipe diameter, type of fitting and soil
305 condition and the *PGV* is the peak ground velocity which has the units in *in/s*. *K* is assumed 0.5,
306 because in Calascibetta are polyethylene pipes and the type of fitting adopted is rubber gasket, while the
307 PGV is assumed equal to 22.5 *cm/s* (8.86 *in/s*). So applying Equation (15), the value of *RR* is equal to
308 0.008. Furthermore, the WDN of Calascibetta consists of pipes of different importance, which have
309 been distinguished in four groups: (1) *main pipes*, (2) *pipes at the entrance of each district*, (3)
310 *connecting pipes* and (4) *plain pipes within each district*. In order to take into account the different
311 importance of each pipe Equation (15) has been modified introducing the importance factor (I_m), thus

312 $$RR = I_{\mathrm{m}} K (0.00187) PGV \quad (16)$$

313 where I_{m} is assumed equal to *2, 1.5, 1* and *0.8*, respectively. Finally, the probability of having a number

314 n of breakages in a pipe of length L is given by the following expression

315 $$P(n) = \frac{(RR \cdot L)^n}{n!} e^{-RR \cdot L} \quad (17)$$

316 where n is the number of pipe breaks, RR the repair ratio evaluated using Equation (16) and L is the

317 length of pipe (expressed in terms of 1000-ft segment USCS). Figure 6 shows the probability of having

318 a certain number of breaks in the WDN of Calascibetta. The figure justifies the choice of selecting the

319 scenarios with a single break, because the probability of having two breaks is negligible.

320

321 **Risk of pipe failure**

322 The risk of failure of a WDN can be obtained using its topology and the failure probability $P(n)$ of every

323 pipe. The failure to deliver a sufficient amount of water from an inflow node i to an outflow node j, can

324 be defined as the probability that the hydraulic head goes below a specified threshold value. Therefore,

325 the probability of failure of a network can be obtained after the hydraulic analysis of a damaged

326 network. Then Monte Carlo simulations are employed reducing the network topology by removing the

327 pipes segments based on the failure probability of every pipe $P(n)$. Once the failed pipes are removed,

328 an algorithm based on Graph Theory can be used to determine whether a path between an inflow and an

329 outflow node exists. For every damaged network created, Monte Carlo simulations have been employed

330 using 5000 runs in order to calculate the statistics of the hydraulic quantities of interest. The procedure

331 is discussed in detail in Fragiadakis and Christodoulou (2014).

332

333 **Selection of scenarios event**

Classical risk analysis has different assumptions, objectives and methods which are not sufficient for resilient design, so the departure from the traditional design practices are needed (Park et al., 2013). Resilience is a dynamic quantity that must be constantly managed and is characterized by a lack of certainty. The uncertainty of potential future disruptions makes the use of scenarios important. In this work, four types of scenarios that cover a wide range of potential occurrences for the WDN of Calascibetta have been selected based on a "*hybrid approach*" which combines Monte Carlo based algorithm with engineering judgment. The Monte Carlo based algorithm allows assessing the preliminary failure probabilities in various locations within the network. The reason for combining the engineering judgment in the approach lies on the topology of the WDN of Calascibetta. The network is divided in 8 districts connected with a main pipe and several connecting pipes.

The main pipe and the connecting ones are important because if they fail, the entire district will remain without water, so additional scenarios have been selected for explicitly assessing their significance. However, the failures within the district of smaller diameter pipes have been also selected.

Four groups of scenarios (S_1, S_2, S_3 and S_4) have been selected to examine the effect of different types of pipe failures. *S* denotes a "Scenario" and the subscript number indicates the group to which each scenario belongs (

Figure 7). In detail, the following groups of scenarios in Table 2 have been analyzed:

1. Group S_1 includes scenarios with one break on the main pipeline and the supply pipe of the St. Peter Tank;
2. Group S_2 includes all scenarios with breaks in the supply pipes of each district;
3. Group S_3 includes all scenarios where the breaks occur in the districts;
4. Group S_4 includes all scenarios where the breaks occur in the connecting pipes.

Within group S_3, the scenarios inside each district have been selected, so that the impact of pressure drop and of the number of users affected is maximized. Typically, eight damaged events for every district have been randomly created, with the exceptions of *District 7* where six scenarios have been selected and *District 1* where 12 scenarios have been selected (the largest district). Figure 8 shows the scenarios considered for *District 6*, while in Figure 9 are plotted the average pressures for each scenario and compared to the average pressure in normal operating conditions. During the selection of the scenarios for every District, generally it is noticed that the peripheral areas inside each District have less influence on the global district pressure when one pipe fails. However, other factors can also affect the scenario selection such as the *topographic features* of the district, the *number of users* and the *valve distribution* etc. For example in District 1, because for almost all the assumed scenarios the average pressure level is the same, the scenario with the highest number of users without water service has been selected.

Recovery time and restoration process

In the case study, the control time T_{LC} is assumed equal to 48 hours which is the time to repair the damaged pipe according to the emergency plan of the Water distribution Provider in the region. According to the information provided by the operator (AcquaEnna S.C.p.A) of the WDN, after the earthquake, the first emergency operations (e.g. isolate the zone where the pipe is damaged) are realized within 1 hour, while the repair operations, if the diameter is less than 600 *mm*, are realized in maximum 12 hours. Additionally other 24 hours has been added, because that is the time necessary to inform in advance the residents of the repair operations. Finally, $T_{R.}$ has been assumed equal to 38 hours (one hour has been added to include the uncertainties) and it is assumed constant for all the simulations.

Numerical results and lesson learned

379 In Table 3 are summarized the resilience indices according to Equation (6), (9) and (13) for the different
380 scenarios selected. In the analyses, it is assumed that the water quality check (e.g. hardness, presence of
381 contaminants, etc.) remains above the standards defined by the law and constant before and after the
382 repair, therefore the index R_3 is not shown in the results. The index R_1 is function of the number of
383 households without water and it is lower in the districts where the pipe failure is selected, while it
384 remains constant in other districts, because the effect of the pipe failure is confined in the district using
385 valves. As expected, the lowest value of R_1 index is obtained with scenario 1, which corresponds to
386 failure in the main pipeline. In this case, the seven districts supplied by the main pipeline, remain
387 without water until the pipeline is repaired. This generates a drop of the function $F_1(t)$ and therefore of
388 R_1. The same observation applies to scenarios 21 and 28 that involve the main pipeline. The index R_2
389 instead is more sensitive than R_1 for the selected scenarios, because is affected by the volume of water
390 loss which is function of the *pipe diameter* and the *location of the breakage*. In fact, if the breakage
391 affects a pipe which provide water to several households, during the repair operation when the pipe is
392 isolated, the water tank level increase and so the value of R_2. For example, during Scenario 1, which
393 corresponds to the main pipeline failure, the entire pipe is isolated and all districts are without water.
394 Consequently, the water level in the tank increases because the seven districts are without water supply,
395 and then the R_2 index increases. Scenario 9 (breakage at the input pipe of district 8) is the worst in term
396 of R_2, because for the particular position of this pipe and for its diameter (110 *mm*), the flow rate loss is
397 about 75 *l/s* and this leads emptying St.Peter Tank. Because both indices are equally important to
398 describe certain scenarios, they have been combined together in a global index R which is the synthesis
399 of the information obtained from R_1 and R_2. Further considerations are necessary for the scenario 18
400 when the Index R_2 is evaluated. In this case, the failure is in the pipe connecting District 1 which is
401 supplied by the Roof Tank and District 2 which is supplied by St.Peter Tank, therefore, the index R_2 is

determined using a weight average which is given in Equation (10) where w_1 and w_2 are weight coefficients of the Roof Tank and St.Peter Tank respectively.

Following the two approaches mentioned in previous section, the weights w_1 =0.3274 and w_2 =0.6726 are determined using the first approach, while w_1 =0.0693 and w_2 =0.9307 are determined using the second approach when they are proportional to the reserve capacity which is 31.62 $m^3$for the Roof tank and 424.82 m^3 for San Peter tank, respectively. However, in all tables and figures the results related to scenario 18 refer to the second approach, which is more general. The sensitivity of the Resilience indicators (R_1, R_2 & R) to the time of the earthquake occurrence during the day is shown in

Figure **10** for the scenario 9. The Resilience Index R_2, instead, doesn't have any significant variations with respect to the earthquake occurrence during the day. Instead, for index R_1, if the earthquake occurs at 1 am and failure corresponds to scenario 9, then St.Peter tank is empty, because of the flow rate loss. However, because in the evening the demand flow is less than the input flow, the tank starts increasing its water level and in 24 hours is able to cover the total demand flow. Instead, if the earthquake occurs at 6 am, the demand flow has its peak and the tank in less than 2 hours decreases its water level until it empties to cover the demand and the flow rate loss. From that moment, the tank remains empty, because the demand flow continues to be higher than the input flow. Only when the output flow is less than the input flow, then the water level starts increasing (

Figure **10**).

Restoration plans

Three different restoration plans have been proposed. The *first restoration plan* involves the closure of the tanks until the entire reserve capacity is recovered. The minimum and the maximum variation of recovery time T_R to restore the full capacity in the tanks for the different scenarios are plotted in Figure

11. Please note that for the scenarios 1, 2, 10, 21, 28 and 29 the recovery time is not shown, because the reserve is automatically recovered during the time interval $T_{LC.}$

The maximum and the minimum recovery time in Figure 11 has been evaluated using the procedure described in Figure 12 for scenario 12 where is plotted the tank water height vs. time (hours) right after the earthquake. The bold line represents the water level in normal operating conditions, while the gray line the water level when no recovery strategies have been applied. At the end of the control time $T_{LC,}$ the final water height h_{Final} will be less than the reserve height $h_{Reserve}$ (4.47 *m* for the Roof Tank, 3.23 *m* for St. Peter Tank). This is happening because in normal operating conditions, the final water height is higher than the water reserve height, because the reserve capacity of the tank is not used. However, when the pipe fails the water reserve capacity of the tank is used to satisfy the water demand, so the final water height will be lower than the water reserve height. The difference between these two values ($\Delta h = h_{Reserve} - h_{Final}$) has led to the construction of the gray dashed line in Figure 12 that is the target to reach for recovering the reserve capacity. In particular, the grey line (No restore) is translated of Δh to have a curve that follows the water demand and that reaches the $h_{Reserve}$ at the end of the 48 hours. The others curves correspond to different instants when the tank is closed. The straight lines derive from the assumption of constant water flow in the tank when it is closed, therefore they can estimate the time interval to recover the reserve capacity and when the entities suffer water outage. For example, for scenario 12, the maximum recovery time is 13 hours and the minimum is 6 hours. The minimum and the maximum recovery time will depend on Δh. With the restoration strategy above, no other costs of electricity due to the use of pumps must be added, but in that time interval, the users remain without water supply.

The *second restoration plan* involves the use of the maximum available flow from the pump station. In normal operating conditions, the input flow to the distribution system is about 5.44 *l/s*.

448 Neglecting the physiological water losses, the input flow in the roof tank is around 1.16 *l/s*, while the
449 input flow in the St.Peter tank is 4.28 *l/s*. In emergency conditions, the pump station can supply a
450 maximum flow of 19 *l/s*. With this flow rate, the recovery times of the reserve capacity have been
451 calculated for the selected scenarios, using the following equation

452 $$\frac{\Delta h \cdot A_T}{\Delta t \cdot \left(Q_e / 1000\right)} = T_R(h) \qquad (18)$$

453 where $\Delta h = h_{Reserve} - h_{Final}$ in *m*, A_T is the tank's area in m^2, Q_e in *l/s* is the available flow to be added to
454 recover the water reserve capacity, Δt is equal to 3600 *s*. In Figure 13 are shown the values of the
455 recovery time T_R for the second restoration plan. In the selected scenarios, the total reserve capacity
456 which is recovered corresponds to the one of St.Peter Tank, that is equal to Q_e = 13.56 l/s, where Q_e=
457 (19-1.16-4.28) = 13.56 *l/s*. Please note that for the scenarios 1, 2, 10, 18 and 28 the recovery time is not
458 shown, because the reserve is automatically recovered. The higher recovery times are obtained for the
459 scenarios with the lowest h_{Final} and consequently the lowest R_2 values. With this strategy, the recovery
460 time T_R is reduced, but the cost of electricity, deriving from the use of pumps is increased.

461 The *third restoration plan* is a hybrid combination of the first two strategies. First, the water tank
462 is closed for the first seven hours in the morning and then part of the available flow is used for
463 recovering the water reserve capacity. The advantage of this restoration plan is based on the limited use
464 of the available flow from the pump station and the reduced amount of downtime for the water tank,
465 which is going to be closed only in the early morning, generating less discomfort for the residents. The
466 available flow Q_e is obtained using the following equation:

467 $$Q_e = \frac{\Delta h \cdot A_T}{\Delta t \cdot T_R} \qquad (19)$$

468 where the recovery time T_R is equal to 7 hours (fixed), while $\Delta h = h_{Reserve} - h_{Final}$ will be higher than the
469 value obtained in the second strategy, because the final water height increases after the closure of the

tank. This strategy can be adopted for those scenarios where the recovery time T_R is higher with respect to the other two strategies. Please note that in the third strategy the recovery time T_R is measured as sum of the period the tank is closed plus the period the pumps are operating. The use of the third restoration strategy produces an increase of the R_2 value, but also produces a decrease on R_1 value caused by the closure of the tank. The combined index R given in Equation (10) does not change with respect to the condition when no retrofit strategies are applied. For example, in *scenario 12* the R_2 for the Minimum Recovery Time (6 hours) is 0.82; the corresponding R_1 is equal to 0.87 and then the combined index R is 0.71, which is the same when no restoration plans are taken into account. In this case, it is recommended to work with only one of the two indices to appreciate the effect of the retrofit strategy proposed. These considerations bring also to the conclusion that the third restoration plan should be used only for scenarios where the recovery time T_R is short (e.g. scenarios 13, 15 and 29). The use of the second or third restoration plan produces an overall improvement of the indices as shown in Figure 13 and Figure 14. In fact, with these strategies the index R_2 improves, while the index R_1 is maintained at the same level in the second strategy, and it undergoes a slight reduction in the third strategy. The improvement of the global index R with respect to the initial condition shows the validity of the selected retrofit strategies (Figure 15).

Between the scenarios selected, *scenario 18* is interesting, because in this case the two tanks (Roof and St.Peter) are working in parallel at the same time. This implies that the three restoration strategies should be applied on the two tanks simultaneously. For the first strategy, the recovery time T_r for the roof tank is between 3 and 9 hours, while for St. Peter tank is between 9 and 15 hours. For the second strategy, using the same weight coefficients described above, the flow in the roof tank and the flow in St.Peter tank are determined as weight average of the maximum available flow Q_e = 13.56 *l/s*. Using the second restoration plan the recovery times are 5 hours and 16 minutes in the roof tank and 3 hours and 40

493 minutes in St. Peter tank. For the third restoration plan, the flow rate necessary to recover the reserve
494 capacity is Q_e is 0.31 *l/s* (h_{Final} = 3.52 *m*) for the Roof tank, while for St.Peter tank Q_e is 5.8 *l/s* (h_{Final} =
495 2.14 *m*).
496 *Scenario 29* requires also attention, because in this case the pipeline that supplies the St. Peter tank fails,
497 so the tank is able to provide water to the distribution system for the first 32 hours, but then it empties
498 before the repair operations finish. In this case, the most suitable restoration strategies are the second
499 and the third one. When the pipeline has been fixed, the incoming maximum available flow permits the
500 restoration of the reserve capacity in the water tank in about 9 hours. For the third restoration plan, the
501 available flow should be equal to 16.78 *l/s*. The restoration plan 1 can not be used, because when the
502 incoming pipe is under repair, no input flow can supply the tank which is closed, and the restoration of
503 the reserve capacity doesn't occur.
504 So the lesson learned is that applying one strategy with respect to the other depends on several
505 considerations such as the cost of electricity, the possibility to use the maximum available flow from the
506 pumps, the extension of the tank downtime and its effects on consumers, etc.. Although all these aspects
507 are very important, they have not been quantified in the selection of the optimal restoration plans and are
508 not been discussed in this paper, but they will be addressed by the authors in future research.

509 **CONCLUDING REMARKS**

510 A new resilience index *R* to measure the performance of a water distribution network (*WDN*) is
511 proposed, which combines both the technical, the environmental and the social dimension of resilience.
512 The metric is based on the combination of three indices which are defined in term of functionality *F(t)*
513 and recovery time T_R. The proposed indicator not only considers the initial losses, but it also attempts to
514 assess the restoration process of the system. The sensitivity analysis of the global resilience index *R* to

different disruptions scenarios in the WDN of a small town in the south of Italy is presented. The numerical results in EPANET have shown the positive effect of the separation in districts of the network and the need to use the indices separately, because in some scenarios have been observed opposite trends. Three different recovery plans have been compared considering the different disruption scenarios using the proposed indices. Between the different restoration plans, the first one corresponding to closing the tank for the entire town should be used with caution, because if the recovery time is long, it can create widespread disservices to the residents. Therefore, it is suggested to use this plan only when the quantity of water loss due to the damage pipes is modest, and consequently the tank can recover its water level in few hours. Instead, the hybrid approach (third strategy) can be adopted for those scenarios where the recovery time T_R is higher with respect to the other two strategies. In fact, it produces both an increment of the R_2 index and a decrease of the R_1 index caused by the closure of the tank. The considerations introduced in this paper need to be further developed and expanded by the researchers and designers who deal with WDNs. In particular the proposed indicator could be easily included into a knowledge based Decision Support System aimed at helping the Governmental agencies in selecting the most appropriate design for WDNs, by incorporating also the environmental and social dimension in the design process.

ACKNOWLEDGMENTS

The research leading to these results has received funding from the European Community's Seventh Framework Programme - Marie Curie International Outgoing Fellowship (IOF) Actions-FP7/2007-2013 under the Grant Agreement n°PIOF-GA-2012-329871 of the project IRUSAT— Improving Resilience of Urban Societies through Advanced Technologies.

REFERENCES

Ambraseys N. N., Douglas, J., Sarma, S. K., and Smit, P. M. (2005). "Equations for the Estimation of Strong Ground Motions from Shallow Crustal Earthquakes Using Data from Europe and the Middle East: Horizontal Peak Ground Acceleration and Spectral Acceleration." *Bulletin of Earthquake Engineering*, 3, 1-53.

American Lifelines Alliance. (April 2001). "Seismic Fragility Formulations for Water Systems PART1-Guidelines." *American Society of Civil Engineers (ASCE).*

Ballantyne, D. B., Berg, E., Kennedy, J. Reneau, R., and Wu, D. (1990). "Earthquake Loss Estimation Modeling of the Seattle Water System." *Technical Report*. Kennedy/Jenks/Chilton, Federal Way, WA, 139p.

Berche, B., von Ferber, C., Holovatch, T., and Holovatch, Y. (2009). "Resilience of public transport networks against attacks." *European Physical Journal B*, 71(1), 125-137.

Bruneau M., Chang S., Eguchi R., Lee G., O'Rourke T., Reinhorn A. M., Shinozuka M., Tierney K., Wallace W., and Winterfelt D. v. *(2003). "*A framework to Quantitatively Assess and Enhance the Seismic Resilience of Communities." *Earthquake Spectra, 19(4), 733-752.*

Cagnan, Z., Davidson, R. A., and Guikema, S. D. (2006). "Post-Earthquake Restoration Planning for Los Angeles Electric Power." *Earthquake Spectra*, 22(3), 589-608.

Chang SE, Shinozuka M. *"*Measuring improvements in the disaster resilience of communities*".* *Earthquake Spectra 2004;20(3):739–55*

Chang, S., McDaniels, T., Fox, J., Dhariwal, R., and Longstaff, H. (2014). "Toward Disaster-Resilient Cities: Characterizing Resilience of Infrastructure Systems with Expert Judgments." *Risk Analysis*, 34(3), 416-434.

Cimellaro GP, Reinhorn AM, Bruneau M. *"*Resilience of a health care facility*" Proceedings of annual meeting of the Asian Pacific network of centers for earthquake engineering research. ANCER. 2005.*

Cimellaro G. P., Reinhorn A. M., Bruneau M. (2010 a). "Framework for analytical quantification of disaster resilience." *Engineering Structures, 32: 11, 3639–3649.*

Cimellaro G. P., Reinhorn A. M., Bruneau M. (2010 b). "Seismic resilience of a hospital system." *Structure and Infrastructure Engineering, 6: 1-2, 127-144.*

Cimellaro, G. P., Reinhorn, A. M., D'Ambrisi, A., and De_Stefano, M. (2011). "Fragility Analysis and Seismic Record Selection." *Journal of Structural Engineering, ASCE*, 137(3), 379-390.

Cimellaro, G. P., and Pique`, M. (2014a). "Seismic Performance of Health care facilities using Discrete Event Simulation Models." Computational Methods, Seismic Protection, Hybrid Testing and Resilience in Earthquake Engineering - A tribute to the research contribution of Prof. Andrei Reinhorn, Editors: Cimellaro G.P. & Nagarajaiah S. & Kunnath S., ed., Springer International Publishing AG, ed., Springer, Netherland, 3311 GX Dordrecht, 250 ISBN: 978-3-319-06393-5.

Cimellaro, G. P., Villa, O., and Bruneau, M. (2014b). "Resilience-Based Design of Natural gas distribution networks." *Journal of Infrastructure Systems, ASCE*, 10.1061/(ASCE)IS.1943-555X.0000204.

Cimellaro, G. P., and Solari, D. (2014c). "Considerations about the optimal period range to evaluate the weight coefficient of coupled resilience index." *Engineering Structures*, 69(2014), 12-24.

Davis, C. A. (2014). "Water System Service Categories, Post-Earthquake Interaction, and Restoration Strategies." *Earthquake Spectra*, 30(4), 1487-1509.

Dorbritz, R. (2011). "Assessing the resilience of transportation systems in case of large-scale disastrous events." The 8th International Conference on Environmental Engineering, Vilnius, Lithuania, 19-20 May 2011, 1070-1076.

582 Fiksel, J. (2003) Designing resilient, sustainable systems. *Environmental Science and Technology*
583 37(23): 5330-39.

584 Fragiadakis M., Christodoulou S.E. (2014) "Seismic Reliability Assessment of Urban Water Network"
585 *Earthquake Engineering and Structural Dynamics*, 43(3), 357-374.
586 GIRAFFE. (2008). "GIRAFFE USER'S MANUAL version 4.2 January 2008." Cornell University,
587 School of Civil & Environmental Engineering, Ithaca, NY.
588 Hwang, H. H. M., Lin, H., and Shinozuka, M. (1998). "Seismic Performance Assessment of Water
589 Distribution Systems." *Journal of Infrastructure Systems*, ASCE, Vol. 4, No. 3, 118- 125.
590 Heaslip, K., Louisell, W. C., Collura, J., and Serulle, N. U. (2010). "A sketch level method for assessing
591 transportation network resiliency to natural disasters and man-made events." The 89th Annual
592 Meeting of the Transportation Research Board, Washington, D.C., U.S.A., 10-14 January 2010.

593 Holling, C. S. (1973) Resilience and Stability of Ecological Systems. *Annual Review of Ecology and*
594 *Systematics* 4: 1-23.
595 I.N.G.V. (2013). "The National Institute of Geophysics and Vulcanology." http://www.ingv.it/en/.
596 Jalal, M. M. (2008). "Performance Measurement of Water Distribution Systems (WDS) - A critical and
597 constructive appraisal of the state-of-the-art," *Master of Applied Science*, University of Toronto,
598 Toronto.

599 Jayaram, N., and Srinivasan, K. (2008). "Performance-based optimal design and rehabilitation of water
600 distribution networks using life cycle costing." *Water Resources Research*, 44(1), W01417.
601 Javanbarg, M.B., Scawthorn, C. and Takada, S. (2008). Priority evaluation of seismic mitigation in
602 pipeline networks using multicriteria analysis fuzzy AHP. *14th World Conference on Earthquake*
603 *Engineering*.

Kim, Y., Song, J., Spencer, B. and Elnashai, A. S. (2010). Seismic risk assessment of complex interacting infrastructures using matrix-based system reliability method. *Tenth International Conference on Structural Safety & Reliability.* 2889-2893.

Markov, I., Grigoriu, M., and O'Rourke, T. D. (1994). "An Evaluation of Seismic Serviceability Water Supply Networks with Application to the San Francisco Auxiliary Water Supply System." *Technical Report NCEER-94-0001*. Multidisciplinary Center for Earthquake Engineering Research, Buffalo, NY.

Miles SB, Chang SE. "Modeling community recovery from earthquakes." *Earthquake Spectra 2006;22(2):439–58*

Mileti, D. (1999). *Disasters by Design: A Reassessment of Natural Hazards in the United States*, Joseph Henry Press (May 18, 1999) Washington D.C.

Miller-Hooks, E., Zhang, X., and Faturechi, R. (2012). "Measuring and maximizing resilience of freight transportation networks." *Computers & Operations Research*, 39(7), 1633-1643.

Ouyang, M., and Duenas-Osorio, L. (2011). "An approach to design interface topologies across interdependent urban infrastructure systems." *Reliability Engineering & System Safety*, 96(11), 1462-1473.

Ouyang, M. (2014). "Review on modeling and simulation of interdependent critical infrastructure systems." *Reliability engineering & System safety*, 121, 43-60.

Panza, G. F., Mura, C. L., Peresan, A., Romanelli, F., and Vaccari, F. (2012). "Seismic Hazard Scenarios as Preventive Tools for a Disaster Resilient Society." *Advances in Geophysics*, 53, 93-165.

Panza, G. F., Peresan, A., and Magrin, A. (2014a). "Neo-deterministic seismic hazard scenarios for Friuli Venezia Giulia and surrounding areas ", ISPRA- Istituto Superiore per la Protezione e la Ricerca Ambientale - Servizio Geologico d'Italia.

Panza G.F., Kossobokov V., Peresan A., Nekrasova A. (2014b). Chapter 12." Why are the standard probabilistic methods of estimating seismic hazard and risks too often wrong?". In: Wyss M, Shroder J (eds) Earthquake Hazard, Risk, and Disasters. Elsevier, London, 309-357.

Park, J., Seager, T. P., Rao, P., Convertino, M., and Linkov, I. (2013). "Integrating risk and resilience approaches to catastrophe management in engineering systems." *Risk Analysis*, 33(3), 356-67.

Prasad, T. D., and Park, N.-S. (2004). "Multiobjective genetic algorithms for design of water distribution networks." *Journal of Water Resource Planning and Management, ASCE*, 130(1), 73-82.

Queiroz, C., Garg, S. K., and Tari, Z. (2013). "A probabilistic model for quantifying the resilience of networked systems." *Ibm Journal of Research and Development*, 57(5).

Rossman, L. A. (2000). "EPANET users manual." *EPA/600/R-00/057*, National Risk Management Research Laboratory, Cincinnati, OH 45268.

Sabetta, F., and Pugliese., A. (1987). "Attenuation of peak horizontal acceleration and velocity from italian strong-motion records." *Bulletin of the Seismological Society of America*, 77(5), 1491-1513.

Shinozuka, M., Hwang, H., and Murata, M. (1992). "Impact on Water Supply of a Seismically Damaged Water Delivery System." *Lifeline Earthquake Engineering in the Central and Eastern US, Technical Council on Lifeline Earthquake Engineering Monograph No.5.* Ballantyne, D. B., ed., ASCE, Reston, VA, 43-57.

Tamvakis, P., and Xenidis, Y. (2013). "Comparative Evaluation of Resilience Quantification Methods for Infrastructure Systems." *Selected Papers from the 26th Ipma (International Project Management Association), World Congress*, 74, 339-348.

Taylor, C. E. (1991). “Seismic Loss Estimation for a Hypothetical Water System.” *Technical Council on Lifeline Earthquake Engineering Monograph No.2*. ASCE, Reston, VA.

Tinebra, A. (2013). "Resilience Based Design of an Urban Water Distribution System " Master of Science Thesis, Politecnico di Torino, Turin.

Todini, E. (2000). "Looped water distribution design using a resilience index based heuristic approach." *Urban Water*, 2(2), 115-122.

Wang, Y., and O’Rourke, T. D. (2008). "Seismic Performance Evaluation of Water Supply Systems." *Technical Report MCEER-08-0015*, The Multidisciplinary Center for Earthquake Engineering Research (MCEER), Buffalo, NY.

LIST OF TABLES

670

671 Table 1-Charateristics of the pressure Reducing Valves

Id. code	Location	D (mm)	Meters Head (m)
PRV1	Via Dranza	63	20.0
PRV2	Via Giudea	63	15.0
PRV3	Via Vita	63	20.0
PRV4	Via Roma	110	20.0
PRV5	Via Maddalena II	110	15.0
PRV6	Via Teatro	63	25.0
PRV7	Via Maddalena II	110	20.0

672

673

674

675 Table 2- Scenarios considered in the analysis

Scenario	District Location & Group	Location	D (mm)	Average Flow loss (l/s)
1	S1_Main Pipeline	Break of DN 160 PE pipe in Via Conte Ruggero	160	90.11
2	S2_District 1	Break of DN 160 PE pipe in Matrice Square	160	180
3	S2_District 2	Break of DN 63 PE pipe in Via Giudea	63	61.4
4	S2_District 3	Break of DN 63 PE pipe in Via Vita	63	48.63
5	S2_District 4	Break of DN 63 PE pipe in Via Nazionale SS 290	63	53.80
6	S2_District 5	Break of DN 110 PE pipe in Via Nazionale SS 290	110	77.35
7	S2_District 6	Break of DN 63 PE pipe in Via Teatro	63	53.82
8	S2_District 7	Break of DN 110 PE pipe in Via Maddalena II	110	48.36
9	S2_District 8	Break of DN 110 PE pipe in Via Nazionale SS 290	110	75
10	S3_District 1	Break of DN 63 PE pipe in Via Itria	63	33.48
11	S3_District 2	Break of DN 110 PE pipe in Via Giudea	110	66.61
12	S3_District 3	Break of DN 63 PE pipe in Via Minavento	63	21.51
13	S3_District 4	Break of DN 63 PE pipe in Via San Antonio	63	24.47
14	S3_District 5	Break of DN 110 PE pipe in Via Maddalena II	110	55.25
15	S3_District 6	Break of DN 63 PE pipe in Via Annunziata	63	29.55
16	S3_District 7	Break of DN 110 PE pipe in Via Maddalena II	110	38.78
17	S3_District 8	Break of DN 110 PE pipe in Via Nazionale SS 290	110	44.54
18	S4_D1-D2	Break of DN 63 PE pipe in Umberto Square	63	58.05
19	S4_D2-D6 (I)	Break of DN 110 PE pipe in Via Roma	110	71.75
20	S4_D2-D6 (II)	Break of DN 110 PE pipe in Via Roma	110	70.29
21	S4_D2-MP	Break of DN 110 PE pipe in Via Nazionale SS 290	110	87.59
22	S4_D3-D6 (I)	Break of DN 63 PE pipe in Via Fontana	63	33.01
23	S4_D3-D6 (II)	Break of DN 63 PE pipe in Via Aquila	63	33.29
24	S4_D3-D8 (I)	Break of DN 63 PE pipe in Via Scarlata	63	31.72
25	S4_D3-D8 (II)	Break of DN 63 PE pipe in Via Scarlata	63	28.49
26	S4_D4-D5	Break of DN 110 PE pipe in Via Chiusa	110	63
27	S4_D4-D8	Break of DN 63 PE pipe in Via Lucchese	63	27.94
28	S4_D6-MP	Break of DN 160 PE pipe in Umberto Square	160	78.04
29	S1_MainPipeline	Braek of DN 110 PE pipe in Via P.D'Aragona	110	4.28

676

677

678

679

680 Table 3- Resilience Index summary for different scenario events

Scenario	R_1	R_2	$R=R_1\times R_2$	Scenario	R_1	R_2	$R=R_1\times R_2$	Scenario	R_1	R_2	$R=R_1\times R_2$
1	0.40	0.69	0.28	**11**	0.92	0.19	0.18	**20**	0.86	0.23	0.20
2	0.79	0.88	0.69	**12**	0.95	0.74	0.71	**21**	0.58	0.64	0.37
3	0.92	0.23	0.21	**13**	0.83	0.83	0.68	**22**	0.84	0.64	0.54
4	0.95	0.31	0.29	**14**	0.93	0.45	0.42	**23**	0.84	0.64	0.54
5	0.82	0.34	0.28	**15**	0.89	0.91	0.81	**24**	0.93	0.60	0.56
6	0.90	0.33	0.30	**16**	0.97	0.56	0.54	**25**	0.94	0.64	0.60
7	0.88	0.31	0.28	**17**	0.92	0.41	0.37	**26**	0.85	0.36	0.30
8	0.97	0.38	0.37	**18**	0.88	0.57	0.5	**27**	0.96	0.65	0.62
9	0.87	0.11	0.10	**19**	0.86	0.23	0.20	**28**	0.42	0.69	0.29
10	0.90	0.59	0.53					**29**	0.78	0.36	0.28

681
682
683
684
685
686
687

688
689 LIST OF FIGURES

712

713

714

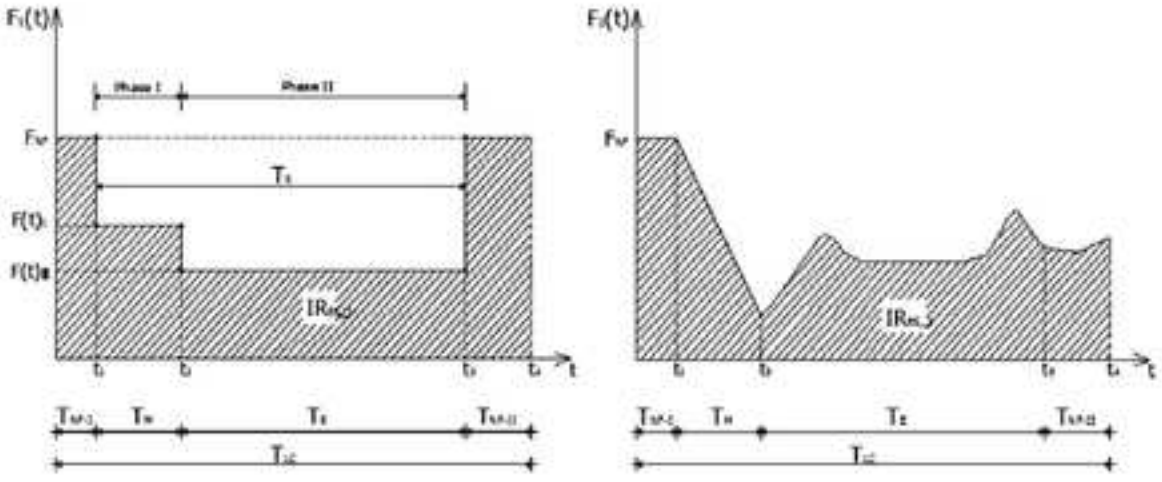

715

716 (a) (b)

717 Figure 1-(a) Functionality of Water Distribution System based on the number of users with suffered
718 water outage and of (b) the tank water height $F_2(t)=h(t)/h_{reserve}$. $IR_{SD,1}$ and $IR_{SD,2}$ represent the area under
719 the functionality curves.

720

721
722
723 Figure 2–Location and overview of Calascibetta Town in Sicily
724

Figure3

Click here to download Figure figure3.eps

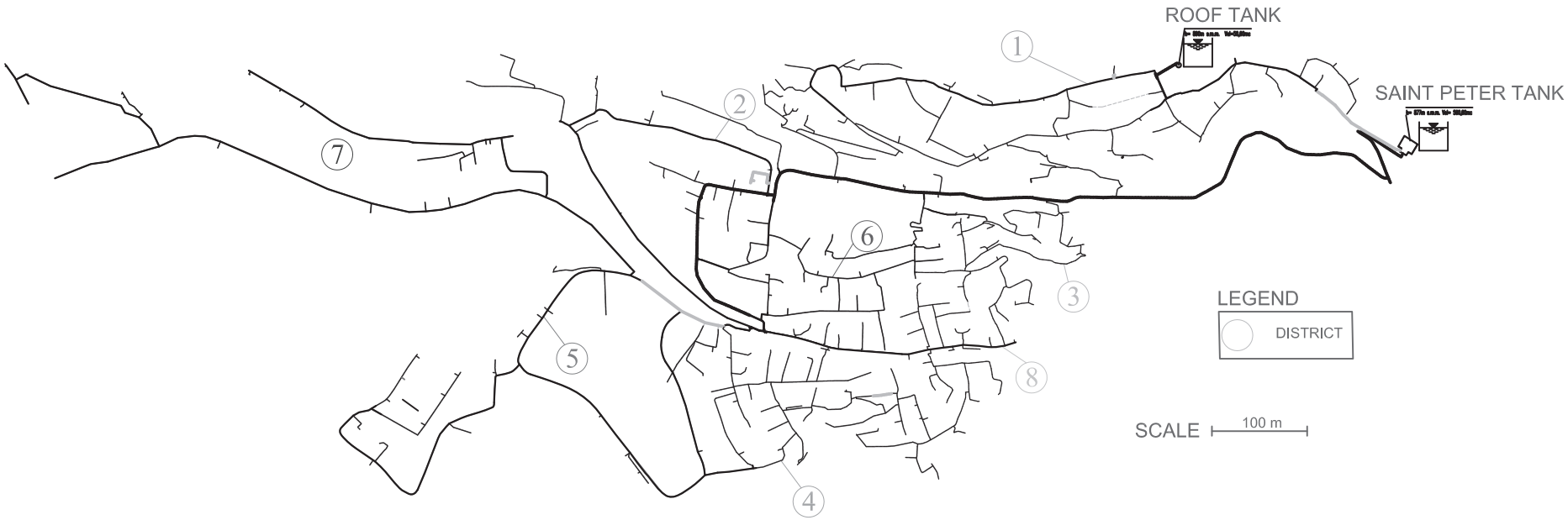

Figure4

Click here to download Figure Figure4.EPS

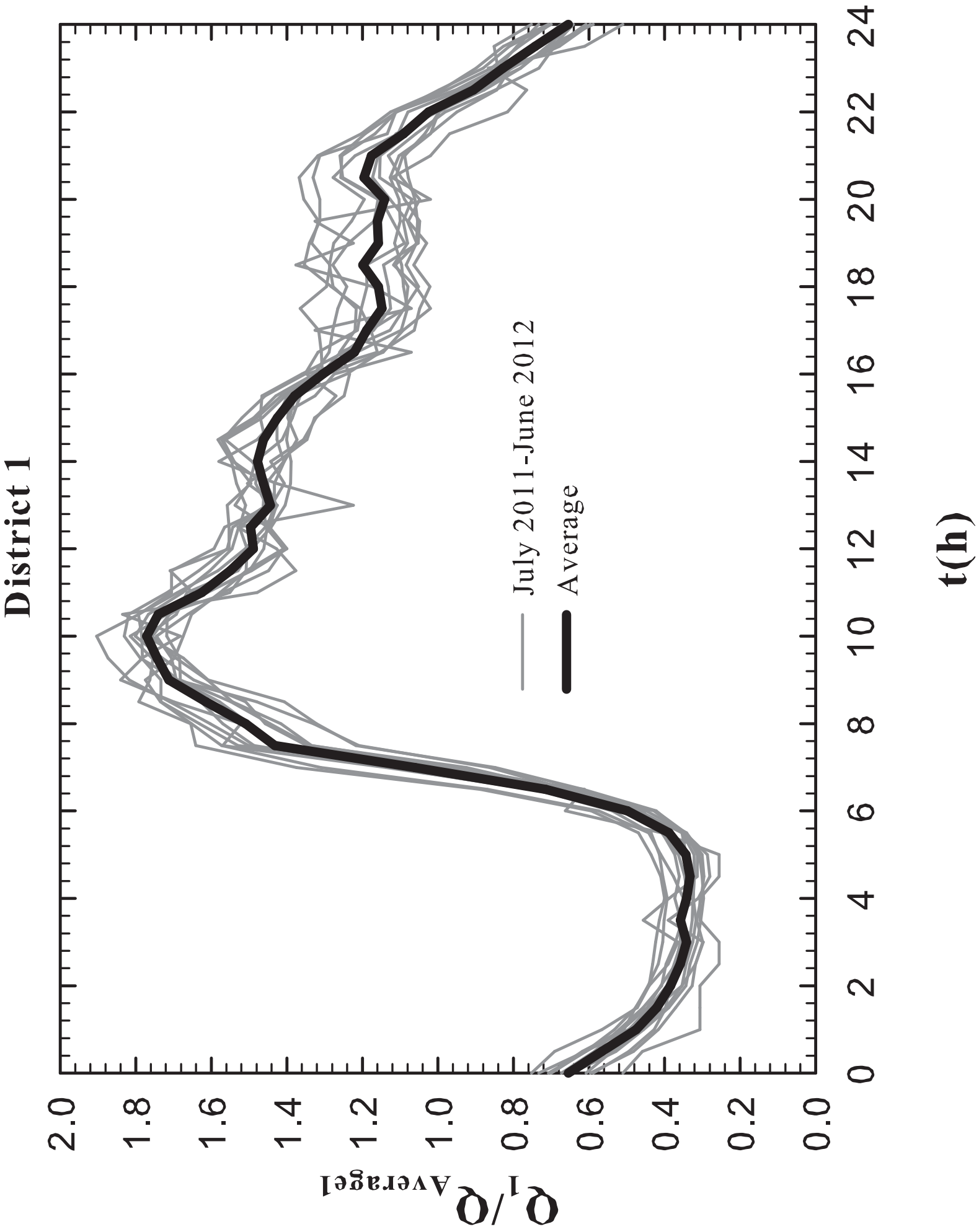

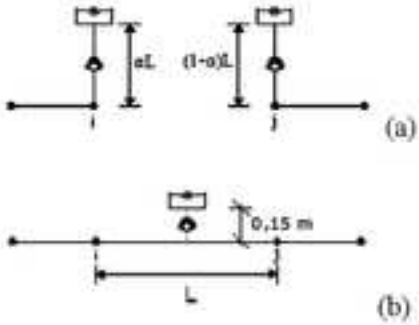

739 Figure 5–Modeling of (a) Pipe Break Simulation and

740 (b) Pipe Leak Simulation in EPANET 2.0 (GIRAFFE, 2008)

741

742

Figure6

Click here to download Figure figure6.EPS

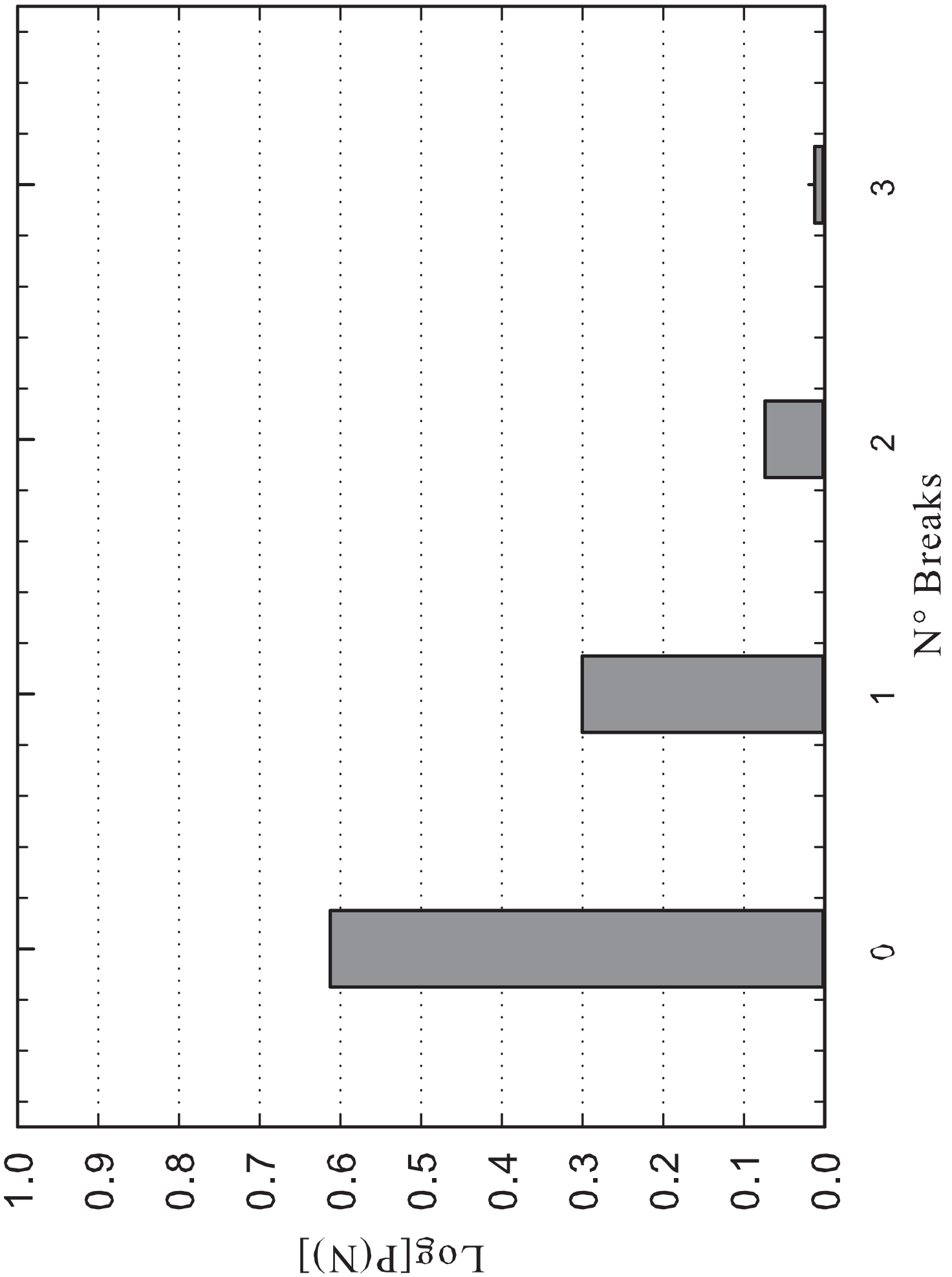

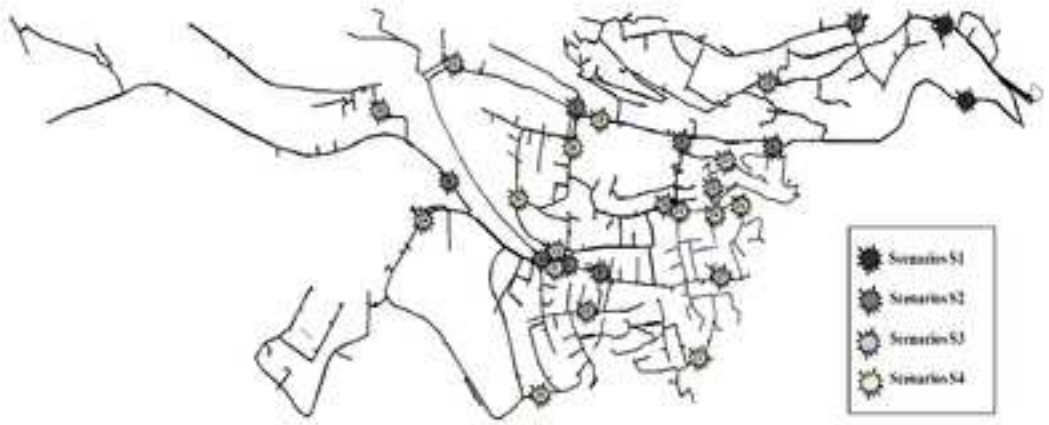

748

749

750 Figure 7-Earthquake Scenarios Event divided by groups

751

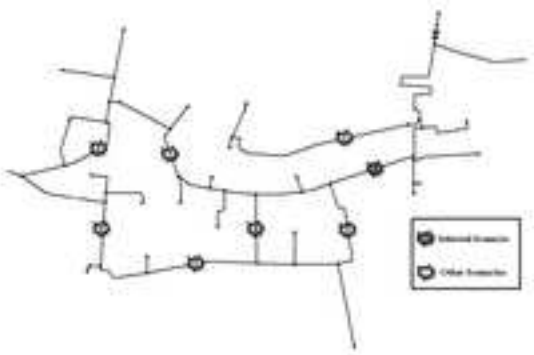

752

753 Figure 8- Scenarios in District 6 for group S3

754

755

756

Figure9

Click here to download Figure figure9.EPS

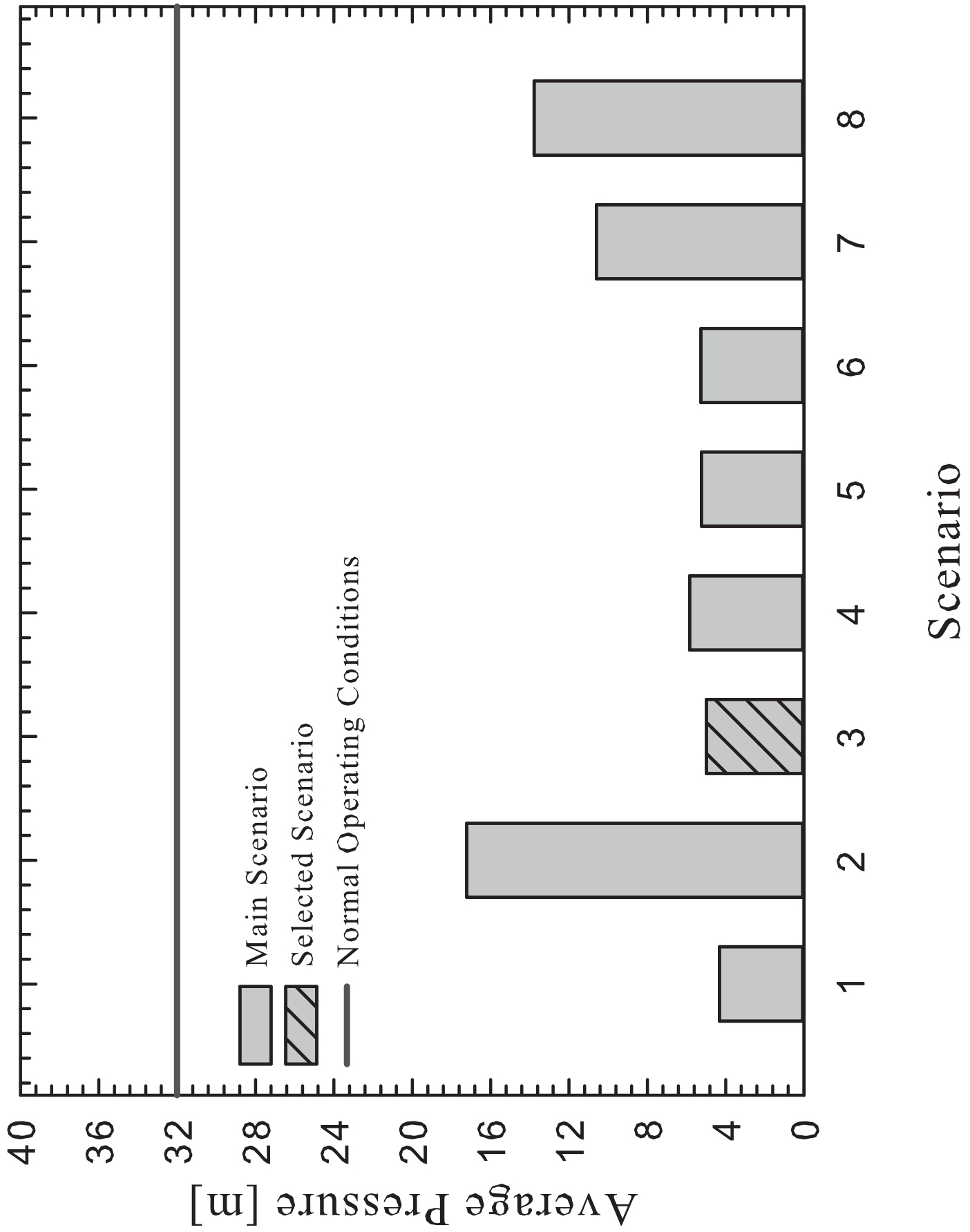

Figure10

Click here to download Figure figure10.EPS

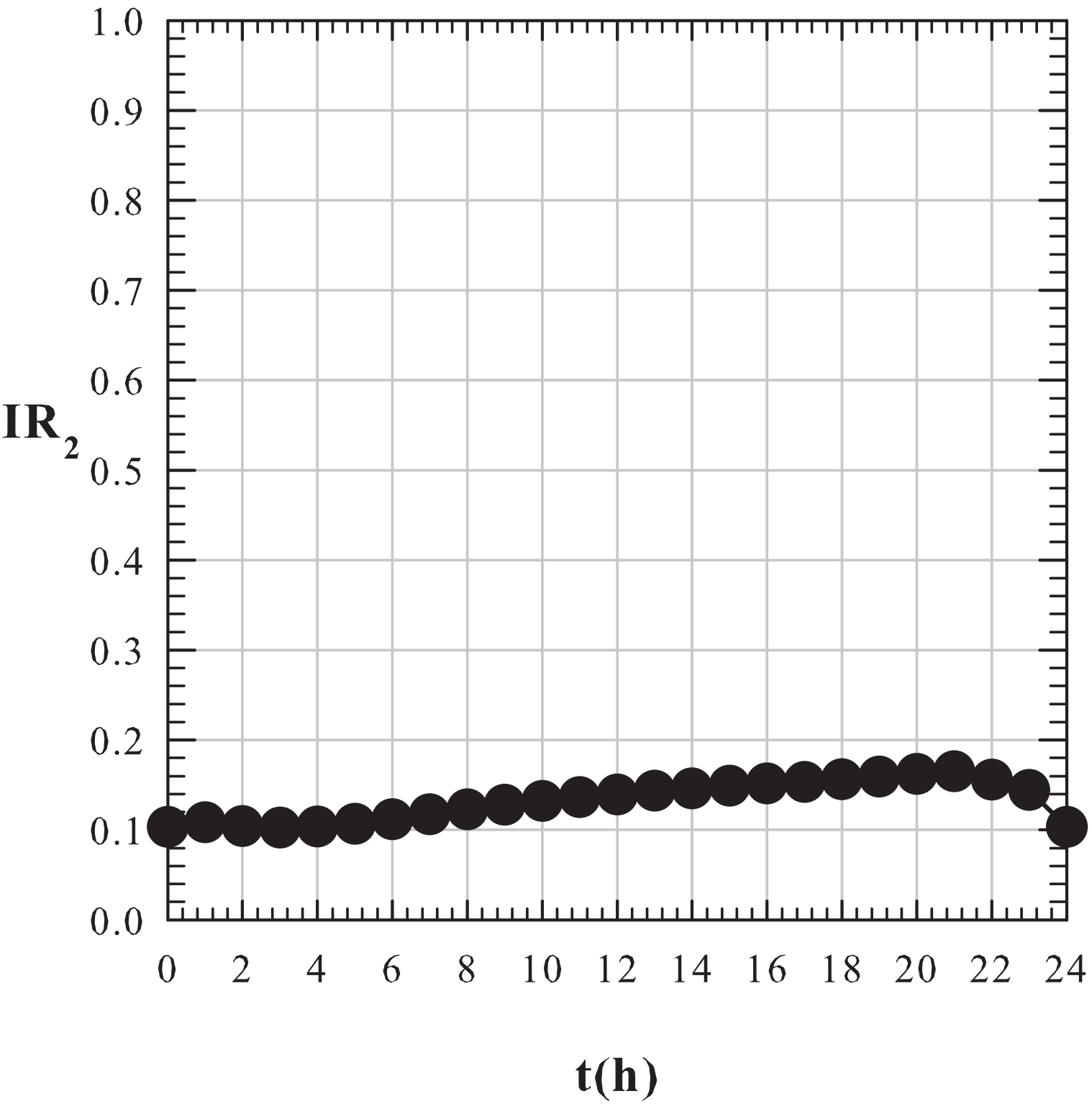

Figure11

Click here to download Figure figure11.EPS

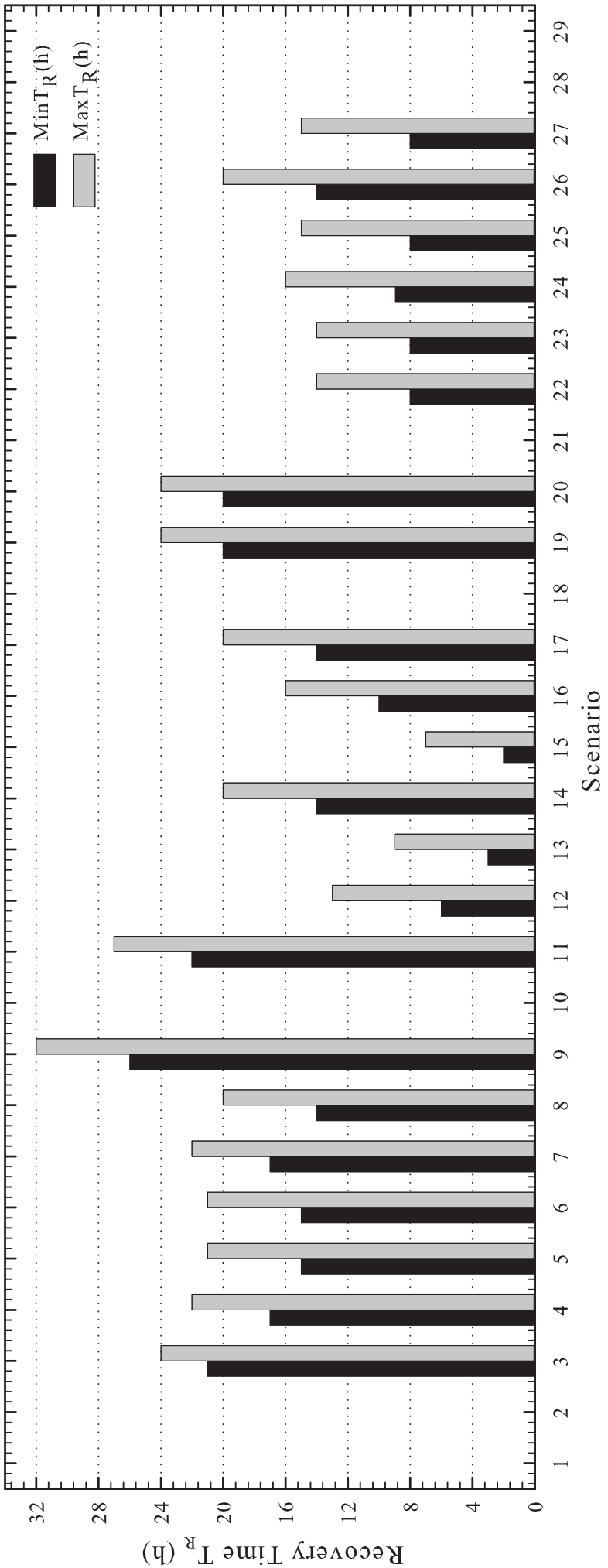

Figure12

Click here to download Figure figure12.EPS

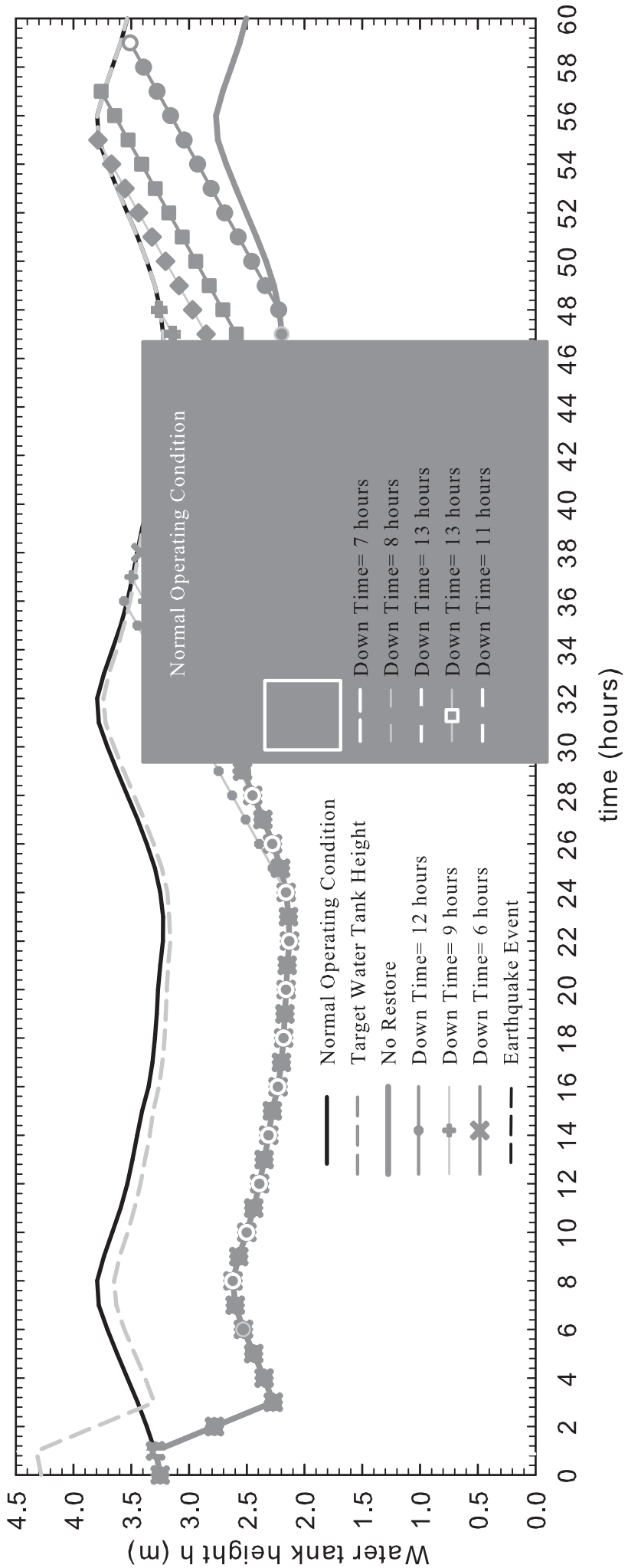

Figure13

Click here to download Figure figure13.EPS

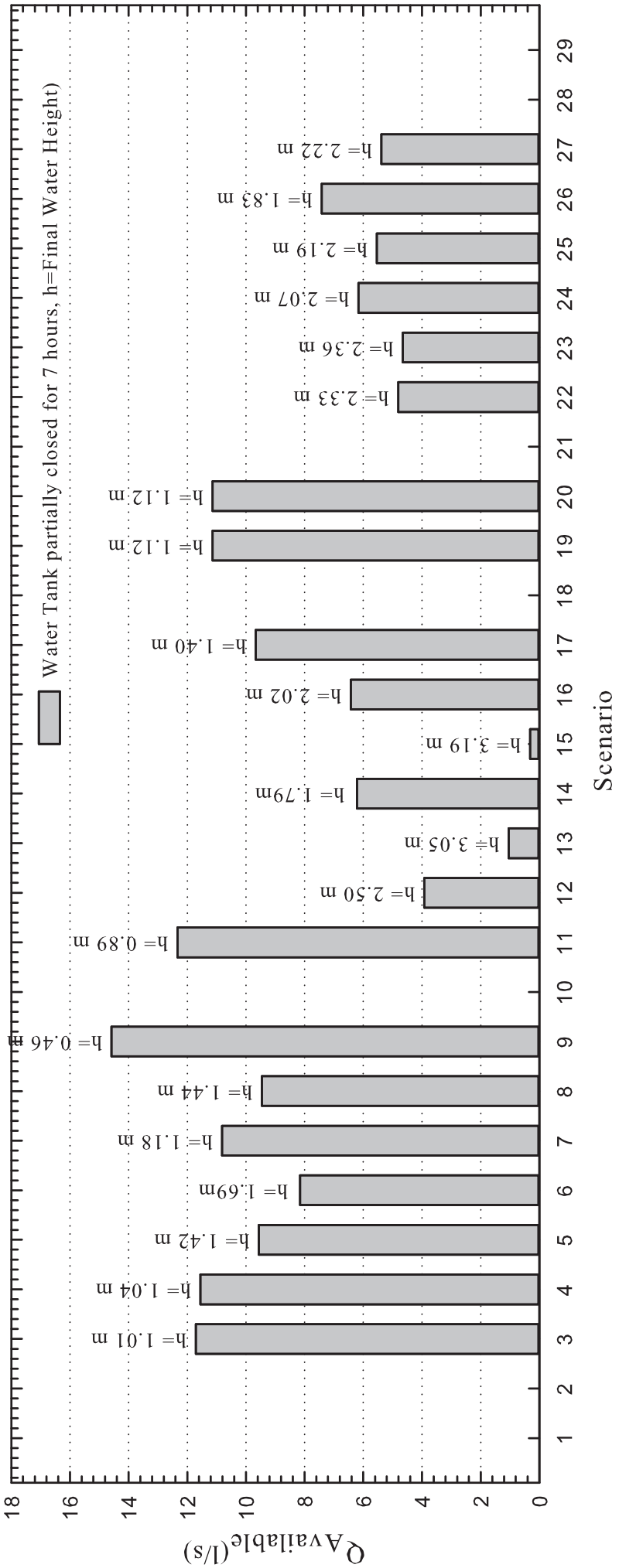

Figure15

Click here to download Figure figure15.EPS